



## **An intranasal lentiviral booster reinforces the waning mRNA vaccine-induced SARS-CoV-2 immunity that it targets to lung mucosa**

Benjamin Vesin, Jodie Lopez, Amandine Noirat, Pierre Authié, Ingrid Fert, Fabien Le Chevalier, Fanny Moncoq, Kirill Nemirov, Catherine Blanc, Cyril Planchais, et al.

### **► To cite this version:**

Benjamin Vesin, Jodie Lopez, Amandine Noirat, Pierre Authié, Ingrid Fert, et al.. An intranasal lentiviral booster reinforces the waning mRNA vaccine-induced SARS-CoV-2 immunity that it targets to lung mucosa. *Molecular Therapy*, 2022, 10.1016/j.ymthe.2022.04.016 . pasteur-03695076

**HAL Id: pasteur-03695076**

**<https://pasteur.hal.science/pasteur-03695076>**

Submitted on 14 Jun 2022

**HAL** is a multi-disciplinary open access archive for the deposit and dissemination of scientific research documents, whether they are published or not. The documents may come from teaching and research institutions in France or abroad, or from public or private research centers.


L'archive ouverte pluridisciplinaire **HAL**, est destinée au dépôt et à la diffusion de documents scientifiques de niveau recherche, publiés ou non, émanant des établissements d'enseignement et de recherche français ou étrangers, des laboratoires publics ou privés.



Distributed under a Creative Commons Attribution - NonCommercial 4.0 International License

# **An intranasal lentiviral booster reinforces the waning mRNA vaccine-induced SARS-CoV-2 immunity that it targets to lung mucosa**

Running title: Boosting mRNA-induced SARS-CoV-2 immunity with a lentiviral-based nasal vaccine

Benjamin Vesin<sup>1,£</sup>, Jodie Lopez<sup>1,£</sup>, Amandine Noirat<sup>1,£</sup>, Pierre Authié<sup>1,£</sup>, Ingrid Fert<sup>1</sup>, Fabien Le Chevalier<sup>1</sup>, Fanny Moncoq<sup>1</sup>, Kirill Nemirov<sup>1</sup>, Catherine Blanc<sup>1</sup>, Cyril Planchais<sup>2</sup>, Hugo Mouquet<sup>2</sup>, Françoise Guinet<sup>3</sup>, David Hardy<sup>4</sup>, Francina Langa Vives<sup>5</sup>, Christiane Gerke<sup>6</sup>, François Anna<sup>1</sup>, Maryline Bourguin<sup>1</sup>, Laleh Majlessi<sup>1,\$,\*</sup>, , and Pierre Charneau<sup>1,\$,\*</sup>

<sup>1</sup> Pasteur-TheraVectys Joint Lab, Institut Pasteur, Virology Department, 28 rue du Dr. Roux, Paris F-75015, France

<sup>2</sup> Laboratory of Humoral Immunology, Université de Paris, Immunology Department, Institut Pasteur, INSERM U1222, Paris F-75015, France

<sup>3</sup> Lymphocytes and Immunity Unit, Université de Paris, Immunology Department, Institut Pasteur, Paris F-75015, France


<sup>4</sup> Histopathology platform, Institut Pasteur, Paris F-75015, France

<sup>5</sup> Mouse Genetics Engineering, Institut Pasteur, Paris F-75015, France

<sup>6</sup> Institut Pasteur, Université de Paris, Innovation Office, Vaccine Programs, Institut Pasteur, Paris F-75015, France

<sup>£</sup>These authors contributed equally

<sup>\$</sup>Senior authors

 Corresponding author: [laleh.majlessi@pasteur.fr](mailto:laleh.majlessi@pasteur.fr)

## **Keywords**

Intranasal Vaccination / Lentiviral Vaccine / SARS-CoV-2 Emerging Variants of Concern / Mucosal Immunity / Mucosal Booster Vaccine / Waning anti-COVID-19 Immunity

## Abstract

As the COVID-19 pandemic continues and new SARS-CoV-2 variants of concern emerge, the adaptive immunity initially induced by the first-generation COVID-19 vaccines starts waning and needs to be strengthened and broadened in specificity. Vaccination by the nasal route induces mucosal, humoral and cellular immunity at the entry point of SARS-CoV-2 into the host organism and has been shown to be the most effective for reducing viral transmission. The lentiviral vaccination vector (LV) is particularly suitable for this route of immunization due to its non-cytopathic, non-replicative and scarcely inflammatory properties. Here, to set up an optimized cross-protective intranasal booster against COVID-19, we generated an LV encoding stabilized Spike of SARS-CoV-2 Beta variant (LV::S<sub>Beta-2P</sub>). mRNA vaccine-primed and -boosted mice, with waning primary humoral immunity at 4 months post-vaccination, were boosted intranasally with LV::S<sub>Beta-2P</sub>. Strong boost effect was detected on cross-sero-neutralizing activity and systemic T-cell immunity. In addition, mucosal anti-Spike IgG and IgA, lung resident B cells, and effector memory and resident T cells were efficiently induced, correlating with complete pulmonary protection against the SARS-CoV-2 Delta variant, demonstrating the suitability of the LV::S<sub>Beta-2P</sub> vaccine candidate as an intranasal booster against COVID-19. LV::S<sub>Beta-2P</sub> vaccination was also fully protective against Omicron infection of the lungs and central nervous system, in the highly susceptible B6.K18-hACE2<sup>IP-THV</sup> transgenic mice.

## Introduction

Considering: (i) the sustained pandemicity of coronavirus disease 2019 (COVID-19), (ii) weakening protection potential of the first-generation vaccines against Severe Acute Respiratory Syndrome beta-coronavirus 2 (SARS-CoV-2), and (iii) the ceaseless emergence of new viral Variants of Concerns (VOCs), new effective vaccine platforms can be critical for future primary or booster vaccines<sup>1</sup>. We recently demonstrated the strong performance of a non-integrative lentiviral vaccination vector (LV) encoding the full-length sequence of Spike glycoprotein (S) from the ancestral SARS-CoV-2 (LV::S), when used in systemic prime followed by intranasal (i.n.) boost in multiple preclinical models<sup>2</sup>. LV::S ensures complete (cross) protection of the respiratory tract against ancestral SARS-CoV-2 and VOCs<sup>3</sup>. In addition, in our new transgenic mice expressing human Angiotensin Converting Enzyme 2 (hACE2) and displaying unprecedented permissiveness of the brain to SARS-CoV-2 replication, an i.n. boost with LV::S is required for full protection of the central nervous system<sup>3</sup>. LV::S is intended to be used as a booster for individuals who already have been vaccinated against and/or infected by SARS-CoV-2, to reinforce and broaden protection against emerging VOCs with immune evasion potential<sup>4</sup>.

Vaccine LVs are non-integrating, non-replicative, non-cytopathic and negligibly inflammatory<sup>5,6</sup>. These vectors are pseudotyped with the heterologous glycoprotein from Vesicular Stomatitis Virus (VSV-G) which confers them a broad tropism for various cell types, including dendritic cells. The latter are mainly non-dividing cells and thus usually hardly permissive to gene transfer. However, LVs possess the crucial ability to efficiently transfer genes to the nuclei of not only dividing but also non-dividing cells, therefore making efficient transduction of non-dividing immature dendritic cells possible. The resulting endogenous antigen expression in dendritic cells, with their unique ability to activate naïve T cells<sup>7</sup>, correlates with a strong induction of high-quality effector and memory T cells<sup>8</sup>. Importantly, the VSV-G pseudo-typing of LVs prevents them from being targets of preexisting vector-specific immunity in humans, which is key in vaccine development<sup>5,6</sup>. The safety of LVs has been established in humans in a phase I/IIa Human Immunodeficiency Virus-1 therapeutic vaccine trial, although the LV used in that clinical trial had been an integrative version<sup>10,11</sup>. Because of their non-cytopathic and non-inflammatory properties<sup>10,11</sup>, LVs are well suited for mucosal vaccination. The i.n. immunization approach is expected to trigger mucosal IgA responses, as well as resident B and T lymphocytes in the respiratory tract<sup>12</sup>. This immunization route has also been shown to be the most effective at reducing SARS-CoV-2 transmission in both hamster and macaque preclinical models<sup>13</sup>. Induction of mucosal immunity by i.n. immunization allows SARS-CoV-2 neutralization, directly at the gateway to the host organism, before it gains access to major infectable anatomical sites<sup>2</sup>.

The duration of the protection conferred by the first generation COVID-19 vaccines is not yet well established, hardly predictable with serological laboratory tests, inconsistent among individuals and against distinct VOCs. Despite high vaccination rates, the current exacerbation of the world-wide pandemic indicates that repeated booster immunizations will be needed to ensure individual and collective immunity against COVID-19. In this context, the safety and potential adverse effects of multiple additional homologous doses of the first generation COVID-19 vaccines, for instance related to allergic reaction to polyethylene glycol (PEG) contained in mRNA vaccines, have to be considered <sup>14</sup>. Importantly, a heterologous prime-boost vaccine delivery method has been proven to be a more successful strategy than the homologous prime-boost approach in numerous preclinical models of various infectious diseases <sup>15-17</sup>. Therefore, new efficient vaccination platforms are of particular interest to develop heterologous boosters against COVID-19. The LV::S vaccine candidate has potential for prophylactic use against COVID-19, mainly based on its powerful capacity to induce not only strong neutralizing humoral responses, but also and most importantly, robust protective T-cell responses which preserve their immune detection of spike from SARS-CoV-2 VOCs, despite the accumulation of escape mutations <sup>3</sup>. The basis for the immunogenicity of LVs is usually the genetic message they deliver to host cells and that encodes the targeted antigen. However, in the particular case of viral envelope proteins used as antigens, that comprise the transmembrane and the tail segments, it cannot be excluded that the LV is pseudotyped by both VSV-G and the viral envelope protein they encode. In the context of LV::SFL, the possible Spike glycoprotein on the LV surface may contribute to the induction of immune responses, in addition to the genetic message which is translated and expressed by the antigen presenting cells. LV::S is remarkably suited to be used, as a heterologous i.n. booster vaccine, to reinforce and broaden protection against the emerging VOCs, while collective immunity in early vaccinated nations is waning a few months after completion of the initial immunizations, and while new waves of infections are on the rise <sup>4</sup>.

In the present study, toward the preparation of a clinical trial, we first generated an LV encoding the down-selected S<sub>CoV-2</sub> of the Beta variant, stabilized by K<sup>986</sup>P and V<sup>987</sup>P substitutions in the S2 domain of S<sub>CoV-2</sub> (LV::S<sub>Beta-2P</sub>). In mice, primed and boosted intramuscularly (i.m.) with mRNA vaccine encoding for the ancestral S<sub>CoV-2</sub> <sup>18,19</sup> and in which the (cross) sero-neutralization potential was progressively decreasing, we investigated the systemic and mucosal immune responses and the protective potential of an i.n. LV::S<sub>Beta-2P</sub> heterologous boost.

## Results

### Antigen design and down-selection of a lead candidate

To select the most suitable S<sub>CoV-2</sub> variant to induce the greatest neutralization breadth based on the known variants, we generated LVs encoding the full length S<sub>CoV-2</sub> from the Alpha, Beta or Gamma SARS-CoV-2 VOCs. C57BL/6 mice ( $n = 5/\text{group}$ ) were primed i.m. (wk 0) and boosted i.m. (wk 3) with  $1 \times 10^8$  TU/mouse of each individual LV and the (cross) neutralization potential of their sera was assessed before boost (wk 3) and after boost (wk 5) against pseudoviruses carrying various S<sub>CoV-2</sub> (Figure 1A). These pseudo-viruses are LV particles that carry the Spike of interest on their surface but do not have the genetic message for Spike and should not be confused with the LV-based vaccine that carries the genetic message encoding Spike. Immunization with LV::S<sub>Alpha</sub> generated appropriate neutralization capacity against S<sub>D614G</sub> and S<sub>Alpha</sub> but not against S<sub>Beta</sub> and S<sub>Gamma</sub> (Figure 1B). Between LV::S<sub>Beta</sub> and LV::S<sub>Gamma</sub>, the former generated the highest cross sero-neutralization potential against S<sub>D614G</sub>, S<sub>Alpha</sub> and S<sub>Gamma</sub> variants. In accordance with previous observations using other vaccination strategies, in the context of immunization with LV, the K<sup>986</sup>P - V<sup>987</sup>P substitutions in the S2 domain of S<sub>CoV-2</sub> improved the (cross) sero-neutralization potential (Figure 1C), probably due to an extended half-life of S<sub>CoV-2-2P</sub><sup>20</sup>.

Taken together these data allowed to down select S<sub>Beta-2P</sub> as the best cross-reactive antigen candidate to be used in the context of LV (LV::S<sub>Beta-2P</sub>) to strengthen the waning immunity previously induced by the first generation COVID-19 vaccines, like mRNA. Although, the comparison between WT and 2P forms was performed here with the D614G sequence, stabilization by the 2P substitution is so well documented<sup>20</sup> that an extrapolation to S<sub>Beta</sub> seemed well founded.

### Follow-up of humoral immunity in mRNA-primed and -boosted mice and effect of LV::S<sub>Beta-2P</sub> i.n. boost

We analyzed the potential of LV::S<sub>Beta-2P</sub> i.n. boost vaccination to strengthen and broaden the immune responses in mice which were initially primed and boosted with mRNA and in which the (cross) sero-neutralization potential was decreasing. C57BL/6 mice were primed i.m. at wk 0 and boosted i.m. at wk 3 with 1 µg/mouse of mRNA (Figure 2A). In mRNA-primed mice, serum anti-S<sub>CoV-2</sub> and anti-RBD IgG were detected at wk 3, increased after mRNA boost as studied at wk 6 and 10, and then decreased at wk 17 in the absence of an additional boost (Figure S1A).

Longitudinal serological follow-up demonstrated that at 3 wks post prime, cross-neutralization activities against both S<sub>D614G</sub> and S<sub>Alpha</sub> were readily detectable (Figure 2B). Cross sero-neutralization was also detectable, although to a lesser degree, against S<sub>Gamma</sub>, but not against

$S_{\text{Beta}}$ ,  $S_{\text{Delta}}$  or  $S_{\text{Delta+}}$ . At wk 6, i.e., 3 wks post boost, cross sero-neutralization activities against all  $S_{\text{CoV-2}}$  variants were detectable, although at significantly lesser extents against  $S_{\text{Beta}}$ ,  $S_{\text{Delta}}$  and  $S_{\text{Delta+}}$ . From wk 6 to wk 10, cross sero-neutralization against  $S_{\text{Beta}}$ ,  $S_{\text{Delta}}$ , or  $S_{\text{Delta+}}$  gradually and significantly decreased. At wk 10, half of the mice lost the cross sero-neutralization potential against  $S_{\text{Beta}}$ ,  $S_{\text{Delta}}$ , or  $S_{\text{Delta+}}$  (Figure 2B).

At wk 15, groups of mRNA-primed and -boosted mice were injected i.m. with 1  $\mu\text{g}$  of mRNA vaccine or PBS. The dose of 1  $\mu\text{g}$  of mRNA per mouse has been demonstrated to be fully protective in mice<sup>21</sup>. In parallel, at this time point, mRNA-primed and -boosted mice received i.n.  $1 \times 10^9$  Transduction Units (TU)/mouse of an empty LV (LV Ctrl) or escalating doses of  $1 \times 10^6$ ,  $1 \times 10^7$ ,  $1 \times 10^8$ , or  $1 \times 10^9$  TU of LV:: $S_{\text{Beta-2P}}$  (Figure 2A). Unprimed, age-matched mice received i.n.  $1 \times 10^9$  TU of LV:: $S_{\text{Beta-2P}}$  or PBS.

In the previously mRNA-primed and -boosted mice, injected at wk 15 with a third dose of mRNA or with  $1 \times 10^8$  or  $1 \times 10^9$  TU of LV:: $S_{\text{Beta-2P}}$ , marked anti- $S_{\text{CoV-2}}$  IgG titer increases were observed (Figure 2C). The titers of anti- $S_{\text{CoV-2}}$  IgA were higher in the mice injected with  $1 \times 10^9$  TU of LV:: $S_{\text{Beta-2P}}$  than those injected with a third 1  $\mu\text{g}$  dose of mRNA vaccine (Figure 2C). In agreement with these results, (cross) sero-neutralization activity increased in a dose-dependent manner with LV:: $S_{\text{Beta-2P}}$  i.n. boost given at wk 15, as studied at wk 17 (Figure 2D). Of note, cross sero-neutralization activity against  $S_{\text{Omicron}}$ -carrying pseudo-viruses was very low in mRNA-primed and -boosted mice injected at week 15 with a third dose of mRNA via i.m. or with  $1 \times 10^8$  TU of LV:: $S_{\text{Beta-2P}}$  via i.n.. At the mucosal level, at this time point, titers of anti- $S_{\text{CoV-2}}$  and anti-RBD IgG in the total lung extracts increased in a dose-dependent manner in LV:: $S_{\text{Beta-2P}}$ -boosted mice, and the titer obtained with the highest dose of LV:: $S_{\text{Beta-2P}}$  was comparable to that after the third 1  $\mu\text{g}$  i.m. dose of mRNA vaccine (Figure S1B). Importantly, significant titers of lung anti- $S_{\text{CoV-2}}$  IgA were only detected in LV:: $S_{\text{Beta-2P}}$ -boosted mice (Figure S1B).

At the lung cellular level, CD19<sup>+</sup> B cells which are class-switched and thus surface IgM/IgD<sup>+</sup> plasma cells, and which express CD38, CD62L, CD73 and CD80, can be defined as lung resident B cells (Brm)<sup>22,23</sup> (Figure 3A). The proportion of these B cells increased in a dose-dependent manner in the lungs of mice boosted i.n. with LV:: $S_{\text{Beta-2P}}$  (Figure 3B). Mucosal anti- $S_{\text{CoV-2}}$  IgA and Brm were barely detectable in the mice boosted i.m. at wk15 with 1  $\mu\text{g}$  of mRNA, which was the single dose of RNA tested in our experiment and thus serves only as indication.

**Systemic and mucosal T-cell immunity after i.n. LV:: $S_{\text{Beta-2P}}$  boost in previously mRNA-primed and -boosted mice**



Mice were primed and boosted with 1 µg mRNA-vaccine and then boosted i.n. at wk15 with escalating doses of LV::S<sub>Beta-2P</sub>, according to the above-mentioned regimen (Figure 2A). At wk 17, i.e., two wks after the late boost, systemic anti-S<sub>CoV-2</sub> T-cell immunity was assessed by IFN-γ-specific ELISPOT in the spleen of individual mice after in vitro stimulation with individual S:256-275, S:536-550 or S:576-590 peptide, encompassing immunodominant S<sub>CoV-2</sub> regions for CD8<sup>+</sup> T cells in H-2<sup>b</sup> mice<sup>2</sup>. Importantly, the weak anti-S CD8<sup>+</sup> T-cell immunity, detectable in the spleens of mRNA-primed-boosted mice at wk 17, largely increased following i.n. boost with 1 × 10<sup>8</sup> and 1 × 10<sup>9</sup> TU of LV::S<sub>Beta-2P</sub>, similarly to the increase after i.m. mRNA boost (Figure 4).

In parallel, in the same animals, the mucosal anti-S<sub>CoV-2</sub> T-cell immunity was assessed by intracellular Tc1 and Tc2 cytokine staining in T cell-enriched fractions from individual mice after in vitro stimulation with autologous bone-marrow-dendritic cells loaded with a pool of S:256-275, S:536-550 and S:576-590 peptides (Figure 5). In previously mRNA-primed and -boosted mice, only a few S<sub>CoV-2</sub>-specific IFN-γ/TNF/IL-2 CD8<sup>+</sup> T-cell responses were detected in the lungs (Figure 5). However, the i.n. administration of LV::S<sub>Beta-2P</sub> boosted, these Tc1 responses in a dose dependent manner. Sizable percentages of these Tc1 cells were induced with 1 × 10<sup>8</sup> or 1 × 10<sup>9</sup> TU of LV::S<sub>Beta-2P</sub>. mRNA (1 µg) i.m. administration had a substantially lower boost effect on mucosal T cells (Figure 5). Tc2 responses (IL-4, IL-5, IL-10 and IL-13) were not detected in any experimental group (Figure S2), as assessed in the same lung T-cell cultures.

Mucosal lung resident memory T cells (Trm), CD8<sup>+</sup> CD44<sup>+</sup> CD69<sup>+</sup> CD103<sup>+</sup> which are one of the best correlates of protection in infectious diseases<sup>24</sup>, were readily detected in the mice boosted i.n. with 1 × 10<sup>8</sup> or 1 × 10<sup>9</sup> TU of LV::S<sub>Beta-2P</sub> (Figure 6A, B). No Trm were detected in the lungs of mice boosted late with 1 µg mRNA i.m..

#### Features of lungs after LV::S<sub>Beta-2P</sub> i.n. administration

To identify the immune cell subsets transduced in vivo by LV after i.n. administration, C57BL/6 mice were immunized i.n. with the high dose of 1 × 10<sup>9</sup> TU of LV::GFP or LV::nano-Luciferase (LV::nLuc) as a negative control. Lungs were collected at 4 days post-immunization and analyzed by cytometry in individual mice. CD45<sup>-</sup> cell subset was devoid of GFP<sup>+</sup> cells. Only very few GFP<sup>+</sup> cells were detected in the CD45<sup>+</sup> hematopoietic cells (Figure S3A-C). The CD45<sup>+</sup> GFP<sup>+</sup> cells were located in a CD11b<sup>hi</sup> subset and in the CD11b<sup>int</sup> CD11c<sup>+</sup> CD103<sup>+</sup> MHC-II<sup>+</sup> (dendritic cells) (Figure S3B).

To evaluate possible lung infiltration after LV i.n. administration, C57BL/6 mice were injected i.n. with the high dose of 1 × 10<sup>9</sup> TU of LV::S<sub>Beta-2P</sub> or PBS as a negative control. Lungs were collected at 1, 3 or 14 days post-injection for histopathological analysis. H&E histological sections



displayed minimal to moderate inflammation, interstitial and alveolar syndromes in both experimental groups, regardless of the three time points investigated. No specific immune infiltration or syndrome was detected in the animals treated i.n. with  $1 \times 10^9$  TU of LV::S<sub>Beta-2P</sub>, compared to PBS (Figure S4A, B).

#### **Protection of lungs in mRNA-primed and -boosted mice, and later boosted i.n. with LV::S<sub>Beta-2P</sub>**

We then evaluated the protective vaccine efficacy of LV::S<sub>Beta-2P</sub> i.n. in mRNA-primed and -boosted mice. At wk 15, mRNA-primed and -boosted mice received i.m. 1 µg of mRNA or PBS. In parallel, mRNA-primed and -boosted mice received i.n.  $1 \times 10^8$  TU of LV::S<sub>Beta-2P</sub> or control empty LV. (Figure 7A). The choice of this dose was based on our previous experience in which this dose was fully effective in protection in homologous LV::S prime-boost regimens<sup>2,3</sup>, even though it does not result in the strongest immune responses. Unvaccinated, age- and sex-matched controls were left unimmunized. Five weeks after the late boost, i.e. at wk 20, all mice were pre-treated with  $3 \times 10^8$  Infectious Genome Units (IGU) of an adenoviral vector serotype 5 encoding hACE2 (Ad5::hACE2)<sup>2</sup> to render their lungs permissive to SARS-CoV-2 replication (Figure 7A). Four days later, mice were challenged with SARS-CoV-2 Delta variant, which at the time of this study, i.e. November 2021, was the dominant SARS-CoV-2 variant worldwide.

At day 3 post infection, primary analysis of the total lung RNA showed that hACE2 mRNA was similarly expressed in all mice after Ad5::hACE2 *in vivo* transduction (Figure 7B). Lung viral loads were then determined at 3 dpi by assessing total E RNA and sub-genomic (Esg) E<sub>CoV-2</sub> RNA qRT-PCR, the latter being an indicator of active viral replication<sup>25-27</sup>. In mice initially primed and boosted with mRNA-vaccine and then injected i.n. with the control LV or i.m. with PBS, no significant protective capacity was detectable (Figure 7C). In contrast, the LV::S<sub>Beta-2P</sub> i.n. boost of the initially mRNA vaccinated mice drastically reduced the total E RNA content of SARS-CoV-2 and no copies of the replication-related Esg E<sub>CoV-2</sub> RNA were detected in this group (Figure 7C). In the group which received a late mRNA i.m. boost, the total E RNA content was also significantly reduced and the content of Esg E<sub>CoV-2</sub> RNA was undetectable in 3 out of 5 in this group.

Therefore, a late LV::S<sub>Beta-2P</sub> heterologous i.n. boost, given at wk 15 after the first injection of mRNA, at the dose of  $1 \times 10^8$  TU/mouse resulted in complete protection, i.e. total absence of viral replication in 100% of animals, against a high dose challenge with SARS-CoV-2 Delta variant.

#### **Full cross-protective capacity of LV::S<sub>Beta-2P</sub> against SARS-CoV-2 Omicron BA.1 variant**

Given the timing of the lengthy preparation of mRNA-primed and -boosted mice, again boosted i.n. with LV::S<sub>Beta-2P</sub> at wk 15 (July-November 2021), and the emergence of the Omicron

variant (December 2021), it was not possible for us to evaluate the anti-Omicron cross-protection potential of LV::S<sub>Beta-2P</sub> used as a late i.n. boost in parallel. However, we evaluated the protective efficacy of LV::S<sub>Beta-2P</sub> in the very sensitive B6.K18-hACE2<sup>IP-THV</sup> transgenic mice, which are prone to SARS-CoV-2 infection in the lung, and in addition display unprecedented brain permissiveness to SARS-CoV-2 replication<sup>3</sup>. B6.K18-hACE2<sup>IP-THV</sup> mice ( $n = 5-8/\text{group}$ ) were primed i.m. with  $1 \times 10^8$  TU/mouse of LV::S<sub>Beta-2P</sub> or an empty LV at wk 0 and then boosted i.n. at wk 3 with the same dose of the same vectors (**Figure 8A**). Mice were then challenged (i.n.) with  $0.3 \times 10^5$  TCID<sub>50</sub> of a SARS-CoV-2 Omicron BA.1 variant<sup>28</sup> at wk 5. Lung and brain viral RNA contents were then determined at day 5 post infection by using Esg E<sub>CoV-2</sub> RNA qRT-PCR. LV::S<sub>Beta-2P</sub> vaccination conferred sterilizing protection against SARS-CoV-2 Omicron in the lungs and brain *versus* high rates of viral replication in the sham-vaccinated controls (**Figure 8B**). Of note, even if 2 mice out of 8 did not show cervical infection with Omicron, the six others showed significant replication in the brain.

Therefore the LV:S<sub>Beta-2P</sub> displays a full cross-protective capacity against the Omicron variant, which is fully comparable to its efficiency against the ancestral<sup>2,3</sup> or the Delta variant.

## Discussion

With the weakly persistent prophylactic potential of the immunity initially induced by the first-generation COVID-19 vaccines, especially against new VOCs, administration of additional vaccine doses becomes essential<sup>1</sup>. As an alternative to additional doses of the same vaccines, combining vaccine platforms in a heterologous prime-boost regimen holds promise for gaining protective efficacy<sup>29</sup>. Compared to homologous vaccine dose administrations, heterologous prime-boost strategies may reinforce more efficiently specific adaptive immune responses and long-term protection<sup>30</sup>. Furthermore, the sequence of the Spike antigen has to be adapted according to the dynamics of SARS-CoV-2 VOC emergence in order to induce the greatest neutralization breadth. Protection against symptomatic SARS-CoV-2 infection is mainly related to sero-neutralizing activity, while CD8<sup>+</sup> T-cell immunity, with their ability to cytolysis virus-infected cells, especially control the virus replication and result in resolution of viral infection<sup>31</sup>. Therefore, an appropriate B- and T-cell vaccine platform, including an adapted S<sub>CoV2</sub> sequence, is of utmost interest at the current step of the pandemic.

The LV-based strategy, is highly efficient, not only in inducing humoral responses but also, and particularly, in establishing high quality and memory T-cell responses<sup>8</sup>. This makes it a suitable platform for a heterologous boost, even if it is also largely efficacious on its own as a primary COVID-19 vaccine candidate<sup>2,3</sup>. Furthermore, LVs are non-cytopathic, non-replicative and scarcely inflammatory. They can thus be used to perform non-invasive i.n. boost to efficiently induce sterilizing mucosal immunity, which protects the respiratory system as well as the central nervous system<sup>2,3</sup>. The i.n. route of vaccination has been shown by several teams to be the best at reducing viral contents in nasal swabs and nasal olfactory neuroepithelium<sup>32,33</sup>, which can contribute to blocking the respiratory chain of SARS-CoV-2 transmission. One of the advantages of LV-based immunization is the induction of strong T-cell immune responses with high cross-reactivity of T-cell epitopes from Spike of diverse VOCs. Therefore, when the neutralizing antibodies fail or wane, the T-cell arm of the response remains largely protective, as we recently described in antibody-deficient, B-cell compromised  $\mu$ MT KO mice<sup>3</sup>. This property is relative to a high-quality and long-lasting T-cell immunity induced against multiple preserved T-cell epitopes, despite the mutations accumulated in the Spike of the emerging VOCs<sup>3</sup>, including the Omicron variant.

In the present study, we down-selected the S<sub>Beta-2P</sub> antigen which induced the greatest neutralization breadth against the main SARS-CoV-2 VOCs and designed a non-integrative LV encoding a stabilized version of this antigen. The induction of highly cross-reactive neutralizing antibodies by SARS-CoV-2 Beta variant has been well documented<sup>34</sup>. The notable ability of S<sub>Beta</sub>

to elicit cross-reactive antibodies correlates with: (i) the shared genetic and structural features of these antibodies, (ii) their preferential use of specific germline sequences, such as VH1-58 and VH4-39, and (iii) their relatively low number of somatic hypermutations. Collectively, it seems that there exists some common paratopes in such S<sub>Beta</sub>-elicited cross-reactive antibodies which interact with the Y501 mutation found in RBD of Alpha, Beta, and Gamma<sup>35</sup>.

In mice primed and boosted with mRNA vaccine (encoding the ancestral S<sub>CoV-2</sub> sequence), with waning (cross) sero-neutralization capabilities, we used escalating doses of LV::S<sub>Beta-2P</sub> for an i.n. late boost. We demonstrated a dose-dependent increase in anti-S<sub>CoV-2</sub> IgG and IgA titers, and a broadened sero-neutralization potential both in the sera and lung homogenates against VOCs. No anti-S<sub>CoV-2</sub> IgA was detected in the lungs of mice injected with the third dose of 1 µg of mRNA given via i.m. injection. Increasing proportions of non-circulating Brm, defined as class-switched surface IgM<sup>+</sup>/IgD<sup>+</sup> plasma cells, with CD38<sup>+</sup> CD73<sup>+</sup> CD62L<sup>+</sup> CD69<sup>+</sup> CD80<sup>+</sup> phenotype<sup>22,23</sup>, were detected in a dose-dependent manner, in the lungs of mice boosted i.n. with LV::S<sub>Beta-2P</sub>.

Spike-specific, effector lung CD8<sup>+</sup> Tc1 cells were largely detected in the initially mRNA-primed and boosted mice which received a late i.n. LV::S<sub>Beta-2P</sub> boost. These lung CD8<sup>+</sup> T cells did not display Tc2 phenotype. Increasing proportions of lung CD8<sup>+</sup> CD44<sup>+</sup> CD69<sup>+</sup> CD103<sup>+</sup> Trm were also detected, in a dose-dependent manner, only in LV::S<sub>Beta-2P</sub> i.n. boosted mice. The systemic CD8<sup>+</sup> T-cell responses against various immunogenic regions of S<sub>CoV-2</sub> were also increased with 1 × 10<sup>8</sup> or 1 × 10<sup>9</sup> TU doses of LV::S<sub>Beta-2P</sub> i.n. boost in the initially mRNA-primed and -boosted mice. The highest i.n. dose of LV::S<sub>Beta-2P</sub> was comparable to the third injection of 1 µg/mouse of mRNA given by i.m. injection. The fact that the i.n. administration of LV::S<sub>Beta-2P</sub> had a substantial boost effect on the systemic T-cell immunity indicates that this boost pathway is not at the expense of the induction of systemic immunity. As we recently determined by epitope mapping and cytometric analysis, LV::S immunization only induced CD8<sup>+</sup> - but not CD4<sup>+</sup> - T cells against S<sub>CoV-2</sub><sup>2</sup>. This results from direct transduction of antigen-presenting cells by LVs and thus efficient antigen routing to the MHC-I machinery but not to the endocytic and MHC-II presentation pathway (our unpublished observation). Furthermore, as LVs are not cytopathic, the initially transduced antigen-presenting cells should not generate marked amounts of cell debris that could be taken up by secondary antigen-presenting cells for MHC-II presentation.

Evaluation of the protection in mRNA-primed and -boosted mice, showed that 20 wk after the first injection of mRNA vaccine, there was no protection detectable in the lungs against infection with the SARS-CoV-2 Delta variant. Importantly, an i.n. boost at wk 15 with the dose of 1 × 10<sup>8</sup> TU/mouse LV::S<sub>Beta-2P</sub> resulted in full inhibition of SARS-CoV-2 replication in the lungs upon challenge with the Delta variant at wk 20. In the mice receiving an 1 µg mRNA i.m. boost at wk

15 the lung SARS-CoV-2 RNA contents was reduced in a statistically comparable manner, albeit without total inhibition of viral replication in all mice.

The lack of protection against the Delta variant infection only four months after the initial systemic prime-boost by mRNA vaccine, as we observed in the preclinical model in this study, may be explained by the weak efficiency of the ancestral S<sub>CoV-2</sub> sequence to induce long-lasting neutralizing antibodies against the recent VOCs. In addition, it can be hypothesized that the adaptive immune memory induced by i.m. mRNA immunization is likely to be localized in secondary lymphoid organs at anatomical sites located far from the upper respiratory tract. In such a context, the extraordinary rapid replication of new VOCs, such as Delta or Omicron, in the upper respiratory tract would not leave enough time for the reactivation of immune memory from remote anatomical sites and the recruitment of the immune arsenal from these sites. In human populations, such scenario would lead to a high possibility of viral replication and variable levels of its transmission, which would prevent the epidemic from being completely contained by mass vaccination through the systemic route.

It is not yet known if a single third booster will extend and maintain the protective potential, or whether semi-regular boosters will be required against COVID-19 in the future. The LV::S<sub>Beta-2P</sub> i.n. boost strengthens the intensity, broadens the VOC cross-recognition, and targets B-and T-cell immune responses to the principal entry point of SARS-CoV-2, that is, to the mucosal respiratory tract of the host organism preventing the infection of main anatomical sites. It is interesting to note that in rodents only a pair of cervical ganglia exists versus a large network of such ganglia in humans <sup>36</sup>. Following i.n. immunization, this anatomical feature in humans may provide an even more consistent site of immune response induction and local memory maintenance, at the vicinity of to the potential site of airway infection. In addition, nasopharynx-associated lymphoid tissue is a powerful defense system composed of: (i) organized lymphoid tissue, i.e., tonsils, and (ii) a diffuse nose-associated lymphoid tissues, where effector and memory B and T lymphocytes are able to maintain long-lasting immunity <sup>37</sup>. This mucosal immune arsenal deserves to be explored in the control of SARS-CoV-2 transmission in the current context of the pandemic. A phase I clinical trial is currently in preparation for the use of i.n. boost by LV::S<sub>Beta-2P</sub> in previously vaccinated humans or in COVID-19 convalescents. Although LVs cause very little or nearly no inflammation <sup>10,11</sup>, to ensure that i.n. vaccination with LV::S<sub>Beta-2P</sub> will not result in brain inflammation, we plan to evaluate the toxicity of the preclinical GMP batch in regulatory preclinical assays. We will pay particular attention to: (i) biodistribution of LV::S<sub>Beta-2P</sub>, to be assessed by PCR, and (ii) histopathology in as many organs as possible, including the brain, after i.n. administration of the

highest dose planned for the clinical trial and according to kinetics pre-established in non-regulatory preclinical experiments.

We have completed a technology transfer to an industrial partner and are now able to produce LVs in large quantities for clinical trials that will be starting soon. After successful completion of phase I trials, we plan to move to fermenter production, which is now possible for LV production in adherent HEK293-T cells. We have also established the high stability of the LVs if appropriate conservation buffers are used. Compared to adenoviral vectors, LVs have the advantage of being only scarcely inflammatory and not being targets of pre-existing immunity in human populations<sup>6,10</sup>. LVs have a particular tropism for dendritic cells, which generates endogenous antigen expression in these antigen presenting cells, whereas adenoviral vectors preferentially target epithelial cells which requires indirect and cross-presentation of antigens. This may be the reason why LVs are effective at much lower doses compared to adenoviral vectors. The doses of  $1 \times 10^8$  or  $1 \times 10^9$  TU are optimal in mice. However, *Mus musculus* species underestimates the efficacy of HIV-based LVs because of restriction factors which reduces the transduction efficiency of LVs in the murine cells. In larger animals such as piglets<sup>38</sup>, horses (our unpublished results) and macaques<sup>39</sup>, as well as in humans<sup>9</sup>, the same range of LV doses are largely effective for the induction of T-cell responses and protection versus  $1 \times 10^{13}$  adenoviral active particles for human vaccination<sup>6</sup>.

## Materials and Methods

### Mice immunization and SARS-CoV-2 infection

Female C57BL/6JRj mice were purchased from Janvier (Le Genest Saint Isle, France), housed in individually-ventilated cages under specific pathogen-free conditions at the Institut Pasteur animal facilities and used at the age of 7 wks. Mice were immunized i.m. with 1 µg/mouse of mRNA-1273 (Moderna) vaccine. The Moderna vaccine was provided by the Institut Pasteur Medical Center. These were leftover unusable vaccines in thawed vials that were not authorized to be pooled for human vaccination and would have been destroyed. Thus, the doses used in this study did not deprive any individual of a vaccine dose during the pandemic. For i.n. injections with LV, mice were anesthetized by i.p. injection of Ketamine (Imalgene, 80 mg/kg) and Xylazine (Rompun, 5 mg/kg). For protection experiments against SARS-CoV-2, mice were transferred into filtered cages in isolator. Four days before SARS-CoV-2 inoculation, mice were pretreated with  $3 \times 10^8$  IGU of Ad5::hACE2 as previously described<sup>2</sup>. Mice were then transferred into a level 3 biosafety cabinet and inoculated i.n. with  $0.3 \times 10^5$  TCID<sub>50</sub> of the Delta variant of SARS-CoV-2 clinical isolate<sup>40</sup> contained in 20 µl. B6.K18-hACE2<sup>IP-THV</sup> mice<sup>3</sup> were primed i.m. and boosted i.n. by LV::S<sub>Beta-2P</sub> and then inoculated with  $0.3 \times 10^5$  TCID<sub>50</sub> of the Omicron BA.1 variant of SARS-CoV-2 clinical isolate<sup>28</sup>. Mice were then housed in filtered cages in an isolator in BioSafety Level 3 animal facilities. The organs recovered from the infected animals were manipulated according to the approved standard procedures of these facilities.

### Ethical approval of animal experimentation

Experimentation on animals was performed in accordance with the European and French guidelines (Directive 86/609/CEE and Decree 87-848 of 19 October 1987) subsequent to approval by the Institut Pasteur Safety, Animal Care and Use Committee, protocol agreement delivered by local ethical committee (CETEA #DAP20007, CETEA #DAP200058) and Ministry of High Education and Research APAFIS#24627-2020031117362508 v1, APAFIS#28755-2020122110238379 v1.

### Construction and production of vaccinal LV::S<sub>Beta-2P</sub>

First, a codon-optimized sequence of Spike from the Ancestral, D614G, Alpha, Beta or Gamma VOCs were synthesized and inserted into the pMK-RQ\_S-2019-nCoV\_S501YV2 plasmid. The S sequence was then extracted by BamHI/XhoI digestion to be ligated into the pFlap lentiviral plasmid between the BamHI and XhoI restriction sites, located between the native human ieCMV promoter and the mutated *atg* starting codon of Woodchuck Posttranscriptional Regulatory Element (WPRES) sequence (Figure S5). To introduce the K<sup>986</sup>P-V<sup>987</sup>P “2P” double mutation in S<sub>D614G</sub> or



$S_{\text{Beta}}$ , a directed mutagenesis was performed by use of Takara In-Fusion kit on the corresponding pFlap plasmids. Various pFlap-ieCMV-S-WPREm or pFlap-ieCMV-S<sub>2P</sub>-WPREm plasmids were amplified and used to produce non-integrative vaccinal LV, as previously described <sup>2,6</sup>. The envelope plasmid, encodes VSV-G under ieCMV promoter and the packaging plasmid contains *gag*, *pol*, *tat* and *rev* genes. The integrase resulting from this plasmid carries a missense amino acid in its catalytic triad, i.e., the D64V mutation, that prevents the integration of viral DNA into the host chromosome. Without integration, the viral DNA remains in an episomal form, very effective for gene expression <sup>2,6</sup>.

#### **Analysis of humoral and systemic T-cell immunity**

Anti-S<sub>CoV-2</sub> IgG and IgA antibody titers were determined by ELISA by use of recombinant stabilized S<sub>CoV-2</sub> or RBD fragment for coating. Neutralization potential of clarified and decompartmented sera or lung homogenates was quantitated by use of lentiviral particles pseudo-typed with S<sub>CoV-2</sub> from diverse variants, as previously described <sup>2,41</sup>.

T-splenocyte responses were quantitated by IFN- $\gamma$  ELISPOT after in vitro stimulation with S:256-275, S:536-550 or S:576-590 synthetic 15-mer peptides which contain S<sub>CoV-2</sub> MHC-I-restricted epitopes in H-2<sup>d</sup> mice <sup>2</sup>. Spots were quantified in a CTL Immunospot S6 ultimate-V Analyser by use of CTL Immunocapture 7.0.8.1 program.

#### **Phenotypic and Functional cytometric analysis of lung immune cells**

Enrichment and staining of lung immune cells were performed as detailed previously <sup>2,3</sup> after treatment with 400 U/ml type IV collagenase and DNase I (Roche) for a 30-minute incubation at 37°C and homogenization by use of GentleMacs (Miltenyi Biotech). Cell suspensions were then filtered through 100  $\mu$ m-pore filters, centrifuged at 1200 rpm and enriched on Ficoll gradient after 20 min centrifugation at 3000 rpm at RT, without brakes. The recovered cells were co-cultured with syngeneic bone-marrow derived dendritic cells loaded with a pool of A, B, C peptides, each at 1  $\mu$ g/ml or negative control peptide at x  $\mu$ g/ml. The following mixture was used to detect lung Tc1 cells: PerCP-Cy5.5-anti-CD3 (45-0031-82, eBioScience), eF450-anti-CD4 (48-0042-82, eBioScience) and APC-anti-CD8 (17-0081-82, eBioScience) for surface staining and BV650-anti-IFN- $\gamma$  (563854, BD), FITC-anti-TNF (554418, BD) and PE-anti-IL-2 (561061, BD) for intracellular staining. The following mixture was used to detect lung Tc2 cells: PerCP-Cy5.5-anti-CD3 (45-0031-82, eBioScience), eF450-anti-CD4 (48-0042-82, eBioScience), BV711-anti-CD8 (563046, BD Biosciences), for surface staining and BV605-anti-IL-4 (504125, BioLegend Europe BV), APC-anti-IL-5 (504306, BioLegend Europe BV), FITC-anti-IL-10 (505006, BioLegend Europe BV), PE-anti-IL-13 (12-7133-81, eBioScience) for intracellular staining. The intracellular

staining was performed by use of the Fix Perm kit (BD), following the manufacturer's protocol. Dead cells were excluded by use of Near IR Live/Dead (Invitrogen). Staining was performed in the presence of FcγII/III receptor blocking anti-CD16/CD32 (BD).

To identify lung resident memory CD8<sup>+</sup> T-cell subsets, a mixture of PerCP-Vio700-anti-CD3 (130-119-656, Miltenyi Biotec), PECy7-CD4 (552775, BD Biosciences), BV510-anti-CD8 (100752, BioLegend), PE-anti-CD62L (553151, BD Biosciences), APC-anti-CD69 (560689, BD Biosciences), APC-Cy7-anti-CD44 (560568, BD Biosciences), FITC-anti-CD103 (11-1031-82, eBiosciences) and yellow Live/Dead (Invitrogen) was used. Lung Brm were studied by surface staining with a mixture of PerCP Vio700-anti-IgM (130-106-012, Miltenyi), and PerCP Vio700-anti-IgD (130-103-797, Miltenyi), APC-H7-anti-CD19 (560143, BD Biosciences), PE-anti-CD38 (102708, BioLegend Europe BV), PE-Cy7-anti-CD62L (ab25569, AbCam), BV711-anti-CD69 (740664, BD Biosciences), BV421-anti-CD73 (127217, BioLegend Europe BV), FITC-anti-CD80 (104705, BioLegend Europe BV and yellow Live/Dead (Invitrogen).

Cells were incubated with appropriate mixtures for 25 minutes at 4°C, washed in PBS containing 3% FCS and fixed with Paraformaldehyde 4% after an overnight incubation at 4°C. Samples were acquired in an Attune NxT cytometer (Invitrogen) and data analyzed by FlowJo software (Treestar, OR, USA).

#### **Determination of viral RNA content in the organs**

Organs from mice were removed and immediately frozen at -80°C on dry ice. RNA from circulating SARS-CoV-2 was prepared from lungs as described previously <sup>2</sup>. Lung homogenates were prepared by thawing and homogenizing in lysing matrix M (MP Biomedical) with 500 µl of PBS using a MP Biomedical Fastprep 24 Tissue Homogenizer. RNA was extracted from the supernatants of organ homogenates centrifuged during 10 min at 2000g, using the Qiagen Rneasy kit. The RNA samples were then used to determine viral RNA content by E-specific qRT-PCR. To determine viral RNA content by Esg-specific qRT-PCR, total RNA was prepared using lysing matrix D (MP Biomedical) containing 1 mL of TRIzol reagent (ThermoFisher) and homogenization at 30 s at 6.0 m/s twice using MP Biomedical Fastprep 24 Tissue Homogenizer. The quality of RNA samples was assessed by use of a Bioanalyzer 2100 (Agilent Technologies). Viral RNA contents were quantitated using a NanoDrop Spectrophotometer (Thermo Scientific NanoDrop). The RNA Integrity Number (RIN) was 7.5-10.0. SARS-CoV-2 E or E sub-genomic mRNA were quantitated following reverse transcription and real-time quantitative TaqMan® PCR, using SuperScript™ III Platinum One-Step qRT-PCR System (Invitrogen) and specific primers and probe (Eurofins), as recently described <sup>3</sup>.

479        **Lung histology**

480        Left lobes from lungs were fixed in formalin and embedded in paraffin. Paraffin sections (5- $\mu$ m  
481        thick) were stained with Hematoxylin and Eosin (H&E). Slides were scanned using the AxioScan  
482        Z1 (Zeiss) system and images were analyzed with the Zen 2.6 software. Histological images were  
483        evaluated according to a score of 0 to 5 (normal, minimal, mild, moderate, marked, severe).

484

1. [https://cdn.who.int/media/docs/default-source/immunization/sage/covid/global-covid-19-vaccination-strategic-vision-for-2022\\_sage-yellow-book.pdf?sfvrsn=4827ec0d\\_5](https://cdn.who.int/media/docs/default-source/immunization/sage/covid/global-covid-19-vaccination-strategic-vision-for-2022_sage-yellow-book.pdf?sfvrsn=4827ec0d_5). (2021).
2. Ku, M.W., Bourguine, M., Authie, P., Lopez, J., Nemirov, K., Moncoq, F., Noirat, A., Vesin, B., Nevo, F., Blanc, C., Souque, P., et al. (2021). Intranasal vaccination with a lentiviral vector protects against SARS-CoV-2 in preclinical animal models. *Cell Host Microbe* 29, 236-249 e236. 10.1016/j.chom.2020.12.010.
3. Ku, M.W., Authie, P., Bourguine, M., Anna, F., Noirat, A., Moncoq, F., Vesin, B., Nevo, F., Lopez, J., Souque, P., Blanc, C., et al. (2021). Brain cross-protection against SARS-CoV-2 variants by a lentiviral vaccine in new transgenic mice. *EMBO Mol Med*, e14459. 10.15252/emmm.202114459.
4. Juno, J.A., and Wheatley, A.K. (2021). Boosting immunity to COVID-19 vaccines. *Nat Med* 27, 1874-1875. 10.1038/s41591-021-01560-x.
5. Hu, B., Tai, A., and Wang, P. (2011). Immunization delivered by lentiviral vectors for cancer and infectious diseases. *Immunol Rev* 239, 45-61. 10.1111/j.1600-065X.2010.00967.x.
6. Ku, M.W., Charneau, P., and Majlessi, L. (2021). Use of lentiviral vectors in vaccination. *Expert Rev Vaccines*, 1-16. 10.1080/14760584.2021.1988854.
7. Guernonprez, P., Gerber-Ferder, Y., Vaivode, K., Bourdely, P., and Helft, J. (2019). Origin and development of classical dendritic cells. *Int Rev Cell Mol Biol* 349, 1-54. 10.1016/bs.ircmb.2019.08.002.
8. Ku, M.W., Authie, P., Nevo, F., Souque, P., Bourguine, M., Romano, M., Charneau, P., and Majlessi, L. (2021). Lentiviral vector induces high-quality memory T cells via dendritic cells transduction. *Commun Biol* 4, 713. 10.1038/s42003-021-02251-6.
9. TheraVectys-Clinical-Trial (2019). Safety, Tolerability and Immunogenicity Induced by the THV01 Treatment in Patients Infected With HIV-1 Clade B and Treated With Highly Active Antiretroviral Therapy (HAART). <https://www.clinicaltrialsregister.eu/ctr-search/search?query=2011-006260-52> 2011-006260-52.
10. Cousin, C., Oberkamp, M., Felix, T., Rosenbaum, P., Weil, R., Fabrega, S., Morante, V., Negri, D., Cara, A., Dadaglio, G., and Leclerc, C. (2019). Persistence of Integrase-Deficient Lentiviral Vectors Correlates with the Induction of STING-Independent CD8(+) T Cell Responses. *Cell Rep* 26, 1242-1257 e1247. 10.1016/j.celrep.2019.01.025.
11. Lopez, J., Anna, F., Authié, P., Pawlik, A., Ku, M.W., Blanc, C., Souque, P., Moncoq, F., Noirat, A., Hardy, D., Sougakoff, W., et al. An optimized lentiviral vector induces CD4+ T-cell immunity and predicts a booster vaccine against tuberculosis. Submitted.
12. Lund, F.E., and Randall, T.D. (2021). Scent of a vaccine. *Science* 373, 397-399. 10.1126/science.abg9857.
13. van Doremalen, N., Purushotham, J.N., Schulz, J.E., Holbrook, M.G., Bushmaker, T., Carmody, A., Port, J.R., Yinda, C.K., Okumura, A., Saturday, G., Amanat, F., et al. (2021). Intranasal ChAdOx1 nCoV-19/AZD1222 vaccination reduces viral shedding after SARS-CoV-2 D614G challenge in preclinical models. *Sci Transl Med* 13. 10.1126/scitranslmed.abh0755.
14. Castells, M.C., and Phillips, E.J. (2021). Maintaining Safety with SARS-CoV-2 Vaccines. *N Engl J Med* 384, 643-649. 10.1056/NEJMra2035343.
15. He, Q., Mao, Q., An, C., Zhang, J., Gao, F., Bian, L., Li, C., Liang, Z., Xu, M., and Wang, J. (2021). Heterologous prime-boost: breaking the protective immune response bottleneck of COVID-19 vaccine candidates. *Emerg Microbes Infect* 10, 629-637. 10.1080/22221751.2021.1902245.
16. Lu, S. (2009). Heterologous prime-boost vaccination. *Curr Opin Immunol* 21, 346-351. 10.1016/j.coi.2009.05.016.
17. Nordstrom, P., Ballin, M., and Nordstrom, A. (2021). Effectiveness of heterologous ChAdOx1 nCoV-19 and mRNA prime-boost vaccination against symptomatic Covid-19 infection in Sweden: A nationwide cohort study. *Lancet Reg Health Eur*, 100249. 10.1016/j.lanepe.2021.100249.
18. Jackson, L.A., Anderson, E.J., Roupheal, N.G., Roberts, P.C., Makhene, M., Coler, R.N., McCullough, M.P., Chappell, J.D., Denison, M.R., Stevens, L.J., Pruijssers, A.J., et al. (2020). An mRNA Vaccine against SARS-CoV-2 - Preliminary Report. *N Engl J Med* 383, 1920-1931. 10.1056/NEJMoa2022483.
19. Wang, F., Kream, R.M., and Stefano, G.B. (2020). An Evidence Based Perspective on mRNA-SARS-CoV-2 Vaccine Development. *Med Sci Monit* 26, e924700. 10.12659/MSM.924700.
20. Walls, A.C., Park, Y.J., Tortorici, M.A., Wall, A., McGuire, A.T., and Veesler, D. (2020). Structure, Function, and Antigenicity of the SARS-CoV-2 Spike Glycoprotein. *Cell* 181, 281-292 e286. 10.1016/j.cell.2020.02.058.
21. Corbett, K.S., Edwards, D.K., Leist, S.R., Abiona, O.M., Boyoglu-Barnum, S., Gillespie, R.A., Himansu, S., Schafer, A., Ziwawo, C.T., DiPiazza, A.T., Dinno, K.H., et al. (2020). SARS-CoV-2 mRNA vaccine design enabled by prototype pathogen preparedness. *Nature* 586, 567-571. 10.1038/s41586-020-2622-0.
22. Barker, K.A., Etesami, N.S., Shenoy, A.T., Arafa, E.I., Lyon de Ana, C., Smith, N.M., Martin, I.M., Goltry, W.N., Barron, A.M., Browning, J.L., Kathuria, H., et al. (2021). Lung-resident memory B cells protect against bacterial pneumonia. *J Clin Invest* 131. 10.1172/JCI141810.
23. Onodera, T., Takahashi, Y., Yokoi, Y., Ato, M., Kodama, Y., Hachimura, S., Kurosaki, T., and Kobayashi, K. (2012). Memory B cells in the lung participate in protective humoral immune responses to pulmonary influenza virus reinfection. *Proc Natl Acad Sci U S A* 109, 2485-2490. 10.1073/pnas.1115369109.

24. Masopust, D., and Soerens, A.G. (2019). Tissue-Resident T Cells and Other Resident Leukocytes. *Annu Rev Immunol* 37, 521-546. 10.1146/annurev-immunol-042617-053214.
25. Chandrashekar, A., Liu, J., Martinot, A.J., McMahan, K., Mercado, N.B., Peter, L., Tostanoski, L.H., Yu, J., Maliga, Z., Nekorchuk, M., Busman-Sahay, K., et al. (2020). SARS-CoV-2 infection protects against rechallenge in rhesus macaques. *Science* 369, 812-817. 10.1126/science.abc4776.
26. Tostanoski, L.H., Wegmann, F., Martinot, A.J., Loos, C., McMahan, K., Mercado, N.B., Yu, J., Chan, C.N., Bondoc, S., Starke, C.E., Nekorchuk, M., et al. (2020). Ad26 vaccine protects against SARS-CoV-2 severe clinical disease in hamsters. *Nat Med* 26, 1694-1700. 10.1038/s41591-020-1070-6.
27. Wolfel, R., Corman, V.M., Guggemos, W., Seilmaier, M., Zange, S., Muller, M.A., Niemeyer, D., Jones, T.C., Vollmar, P., Rothe, C., Hoelscher, M., et al. (2020). Virological assessment of hospitalized patients with COVID-2019. *Nature* 581, 465-469. 10.1038/s41586-020-2196-x.
28. Planas, D., Saunders, N., Maes, P., Guivel-Benhassine, F., Planchais, C., Buchrieser, J., Bolland, W.H., Porrot, F., Staropoli, I., Lemoine, F., Pere, H., et al. (2022). Considerable escape of SARS-CoV-2 Omicron to antibody neutralization. *Nature* 602, 671-675. 10.1038/s41586-021-04389-z.
29. Barros-Martins, J., Hammerschmidt, S.I., Cossmann, A., Odak, I., Stankov, M.V., Morillas Ramos, G., Dopfer-Jablonka, A., Heidemann, A., Ritter, C., Friedrichsen, M., Schultze-Florey, C., et al. (2021). Immune responses against SARS-CoV-2 variants after heterologous and homologous ChAdOx1 nCoV-19/BNT162b2 vaccination. *Nat Med* 27, 1525-1529. 10.1038/s41591-021-01449-9.
30. Kardani, K., Bolhassani, A., and Shahbazi, S. (2016). Prime-boost vaccine strategy against viral infections: Mechanisms and benefits. *Vaccine* 34, 413-423. 10.1016/j.vaccine.2015.11.062.
31. Sette, A., and Crotty, S. (2021). Adaptive immunity to SARS-CoV-2 and COVID-19. *Cell* 184, 861-880. 10.1016/j.cell.2021.01.007.
32. Bricker, T.L., Darling, T.L., Hassan, A.O., Harastani, H.H., Soung, A., Jiang, X., Dai, Y.N., Zhao, H., Adams, L.J., Holtzman, M.J., Bailey, A.L., et al. (2021). A single intranasal or intramuscular immunization with chimpanzee adenovirus-vectored SARS-CoV-2 vaccine protects against pneumonia in hamsters. *Cell Rep* 36, 109400. 10.1016/j.celrep.2021.109400.
33. Hassan, A.O., Feldmann, F., Zhao, H., Curiel, D.T., Okumura, A., Tang-Huau, T.L., Case, J.B., Meade-White, K., Callison, J., Chen, R.E., Lovaglio, J., et al. (2021). A single intranasal dose of chimpanzee adenovirus-vectored vaccine protects against SARS-CoV-2 infection in rhesus macaques. *Cell Rep Med* 2, 100230. 10.1016/j.xcrm.2021.100230.
34. Moyo-Gwete, T., Madzivhandila, M., Makhado, Z., Ayres, F., Mhlanga, D., Oosthuysen, B., Lambson, B.E., Kgagudi, P., Tegally, H., Iranzadeh, A., Doolabh, D., et al. (2021). Cross-Reactive Neutralizing Antibody Responses Elicited by SARS-CoV-2 501Y.V2 (B.1.351). *N Engl J Med* 384, 2161-2163. 10.1056/NEJMc2104192.
35. Reincke, S.M., Yuan, M., Kornau, H.C., Corman, V.M., van Hoof, S., Sanchez-Sendin, E., Ramberger, M., Yu, W., Hua, Y., Tien, H., Schmidt, M.L., et al. (2022). SARS-CoV-2 Beta variant infection elicits potent lineage-specific and cross-reactive antibodies. *Science* 375, 782-787. 10.1126/science.abm5835.
36. <https://teachmeanatomy.info/neck/vessels/lymphatics/>.
37. Porzia, A., Cavaliere, C., Begvarfaj, E., Masieri, S., and Mainiero, F. (2018). Human nasal immune system: a special site for immune response establishment. *J Biol Regul Homeost Agents* 32, 3-8.
38. de Wispelaere, M., Ricklin, M., Souque, P., Frenkiel, M.P., Paulous, S., Garcia-Nicolas, O., Summerfield, A., Charneau, P., and Despres, P. (2015). A Lentiviral Vector Expressing Japanese Encephalitis Virus-like Particles Elicits Broad Neutralizing Antibody Response in Pigs. *PLoS Negl Trop Dis* 9, e0004081. 10.1371/journal.pntd.0004081.
39. Beignon, A.S., Mollier, K., Liard, C., Coutant, F., Munier, S., Riviere, J., Souque, P., and Charneau, P. (2009). Lentiviral vector-based prime/boost vaccination against AIDS: pilot study shows protection against Simian immunodeficiency virus SIVmac251 challenge in macaques. *J Virol* 83, 10963-10974. 10.1128/JVI.01284-09.
40. Planas, D., Veyer, D., Baidaliuk, A., Staropoli, I., Guivel-Benhassine, F., Rajah, M.M., Planchais, C., Porrot, F., Robillard, N., Puech, J., Prot, M., et al. (2021). Reduced sensitivity of SARS-CoV-2 variant Delta to antibody neutralization. *Nature* 596, 276-280. 10.1038/s41586-021-03777-9.
41. Sterlin, D., Mathian, A., Miyara, M., Mohr, A., Anna, F., Claer, L., Quentric, P., Fadlallah, J., Devilliers, H., Ghillani, P., Gunn, C., et al. (2021). IgA dominates the early neutralizing antibody response to SARS-CoV-2. *Sci Transl Med* 13. 10.1126/scitranslmed.abd2223.

## Acknowledgments

The authors are grateful to Dr. Marie José Quentin-Millet and Estelle Besson (TheraVectys) for precious discussion and advices, to Magali Tichit et Sabine Maurin for excellent technical assistance in preparing histological sections, to Sébastien Chardenoux for excellent technical assistance in B6.K18-hACE2<sup>IP-THV</sup> mouse transgenesis, to Marie Laure Lorient and Dr. Paul-Henri Consigny (Institut Pasteur Medical Center) for their gift of the leftover Moderna vaccines, not unusable in humans in a way that this study did not deprive any individual of a vaccine dose during the COVID-19 pandemic. The SARS-CoV2 variant Delta/2021/I7.2 200 was supplied by the Virus and Immunity Unit (Institut Pasteur, Paris, France) headed by Olivier Schwartz. The SARS-CoV-2 Omicron BA.1 variant was initially supplied by the Virus and Immunity Unit (Institut Pasteur, Paris, France) headed by Olivier Schwartz, and was provided to our lab by Matthieu Prot and Etienne Simon-Lorière (G5 Evolutionary Genomics of RNA Viruses, Institut Pasteur, Paris, France).

This work was supported by TheraVectys and Institut Pasteur.

## Author Contributions

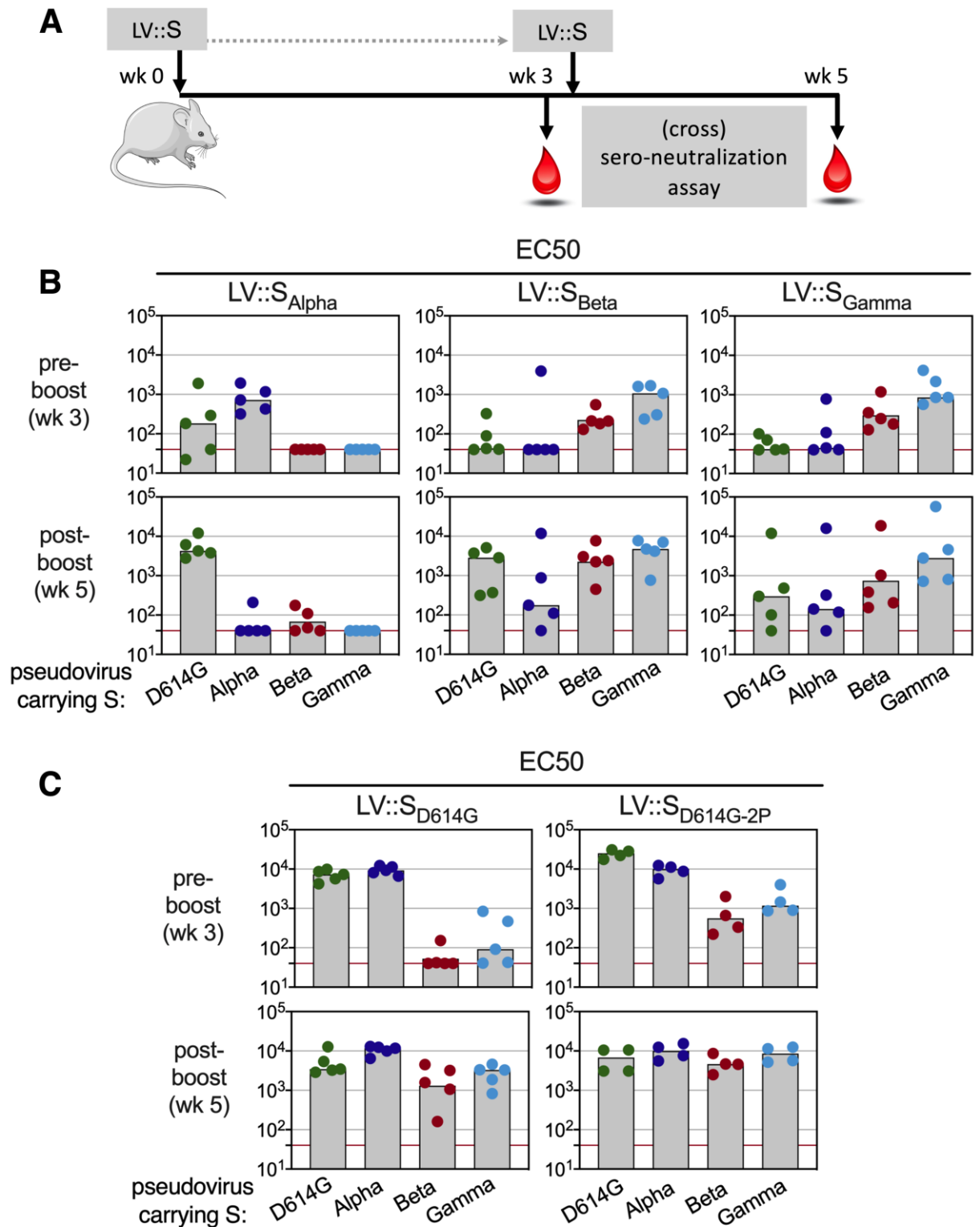
Study concept and design: BV, JL, CG, MB, LM, PC, acquisition of data: BV, JL, AN, PA, IF, FLC, FM, KN, MB, LM, construction and production of LV and technical support: AN, FM, CB, FA, histology: FG, DH, recombinant Spike protein: CP, HM, collaborative generation of B6.K18-hACE2<sup>IP-THV</sup> transgenic mice: FLV, analysis and interpretation of data: BV, JL, FA, MB, LM, PC, drafting of the manuscript: LM.

## Conflict of Interests

PC is the founder and CSO of TheraVectys. BV, AN, PA, IF, FLC, FM, KN and FA are employees of TheraVectys. LM has a consultancy activity for TheraVectys. Other authors declare no competing interests. PA, IF, JL, BV, FA, MB, LM and PC are inventors of pending patents directed to the potential of i.n. LV::S vaccination against SARS-CoV-2.

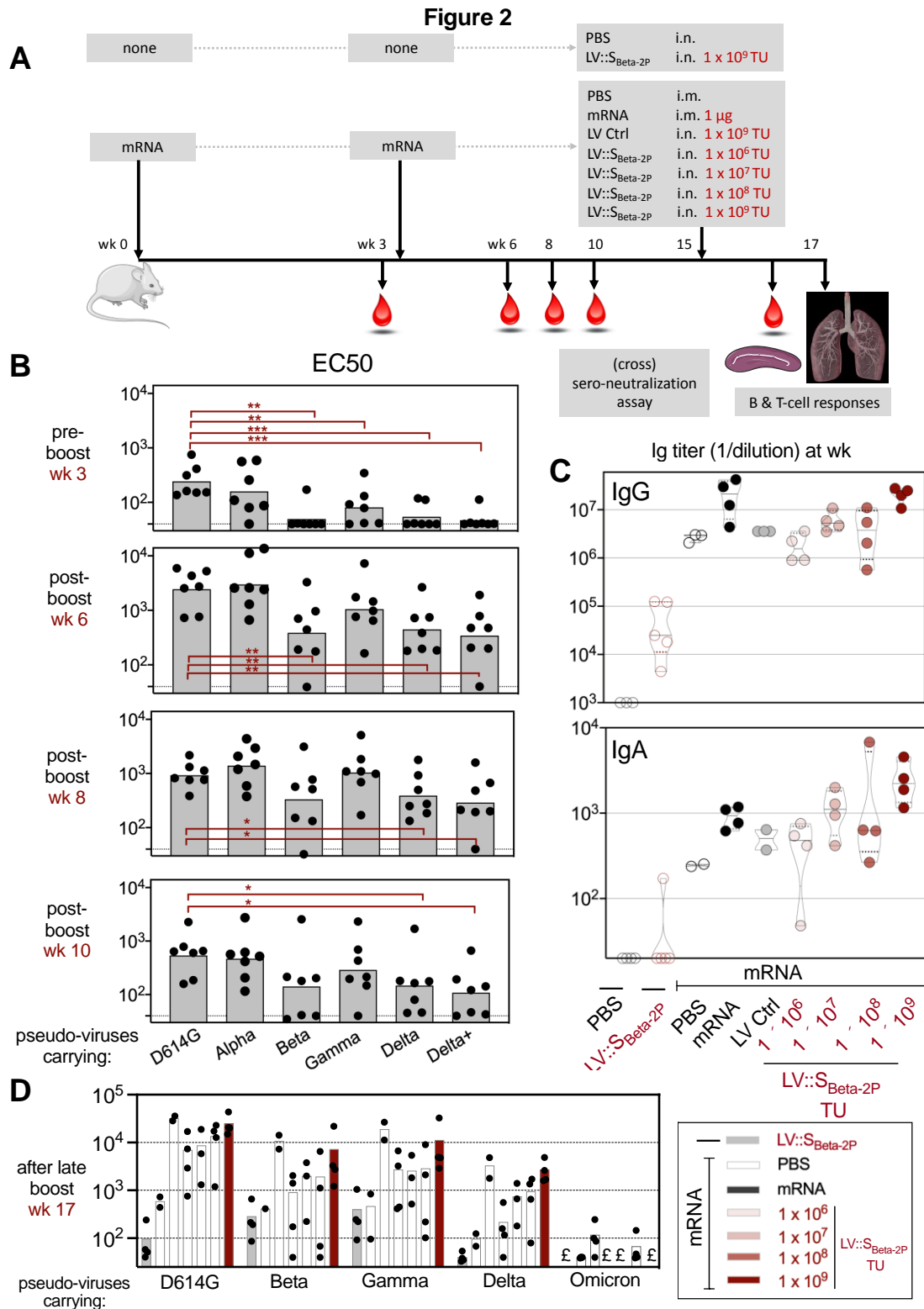


Figure 1



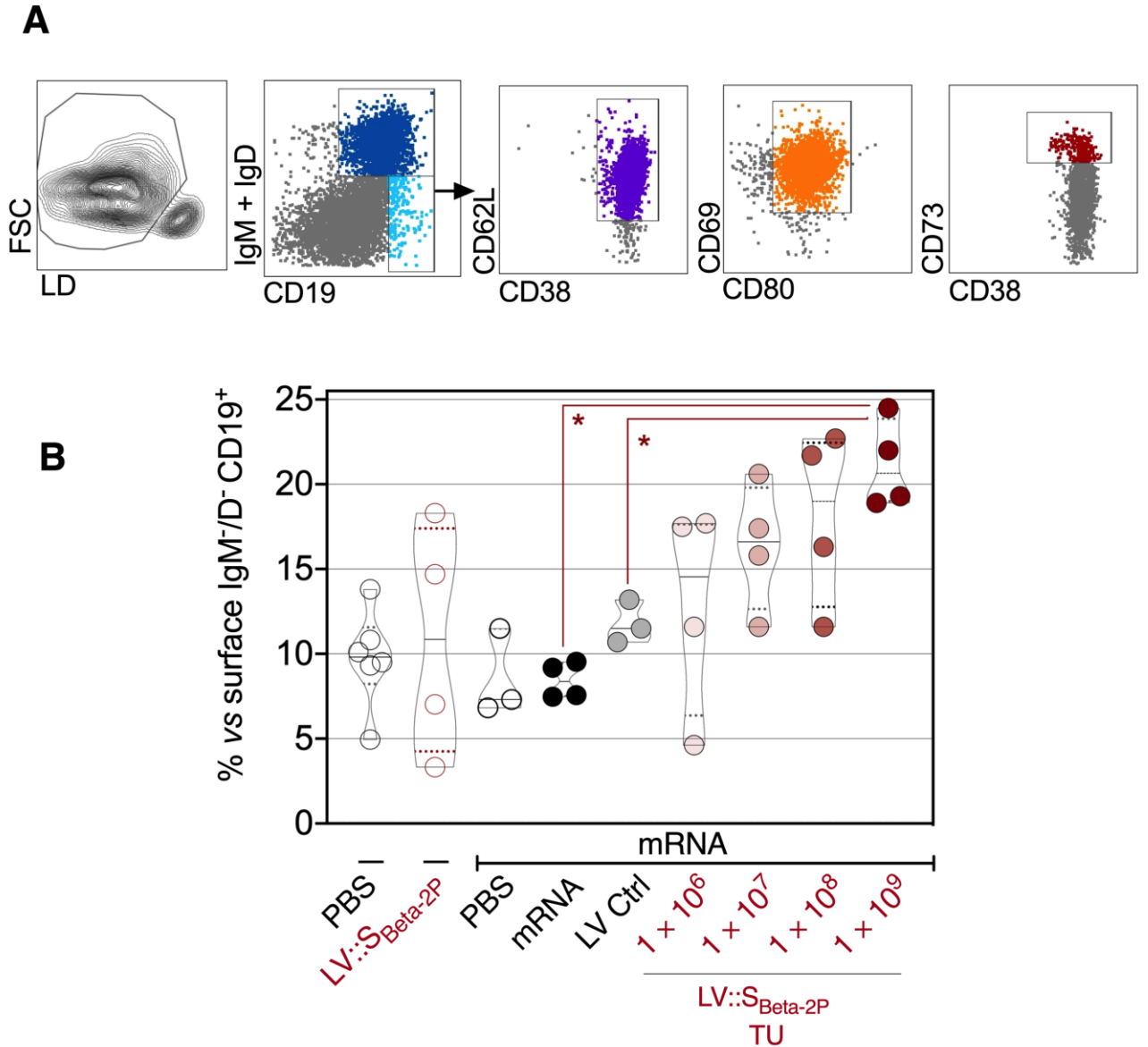
**Figure 1. Down-selection of a S<sub>CoV-2</sub> variant with the highest potential to induce cross sero-neutralizing antibodies.** (A) Timeline of prime-boost vaccination with LV::S<sub>Alpha</sub>, LV::S<sub>Beta</sub> or LV::S<sub>Gamma</sub> and (cross) sero-neutralization assays in C57BL/6 mice ( $n = 4-5/\text{group}$ ). (B) EC50 of neutralizing activity of sera from vaccinated mice was evaluated before and after the boost, against pseudo-viruses carrying S<sub>CoV-2</sub> from D614G, Alpha, Beta or Gamma variants. (C) EC50 of sera from C57BL/6 mice, vaccinated following the regimen detailed in (A) with LV encoding for S<sub>D614G</sub>, either WT or carrying the K<sup>986</sup>P - V<sup>987</sup>P substitutions in the S2 domain. EC50 was evaluated before and after the boost, as indicated in (B).





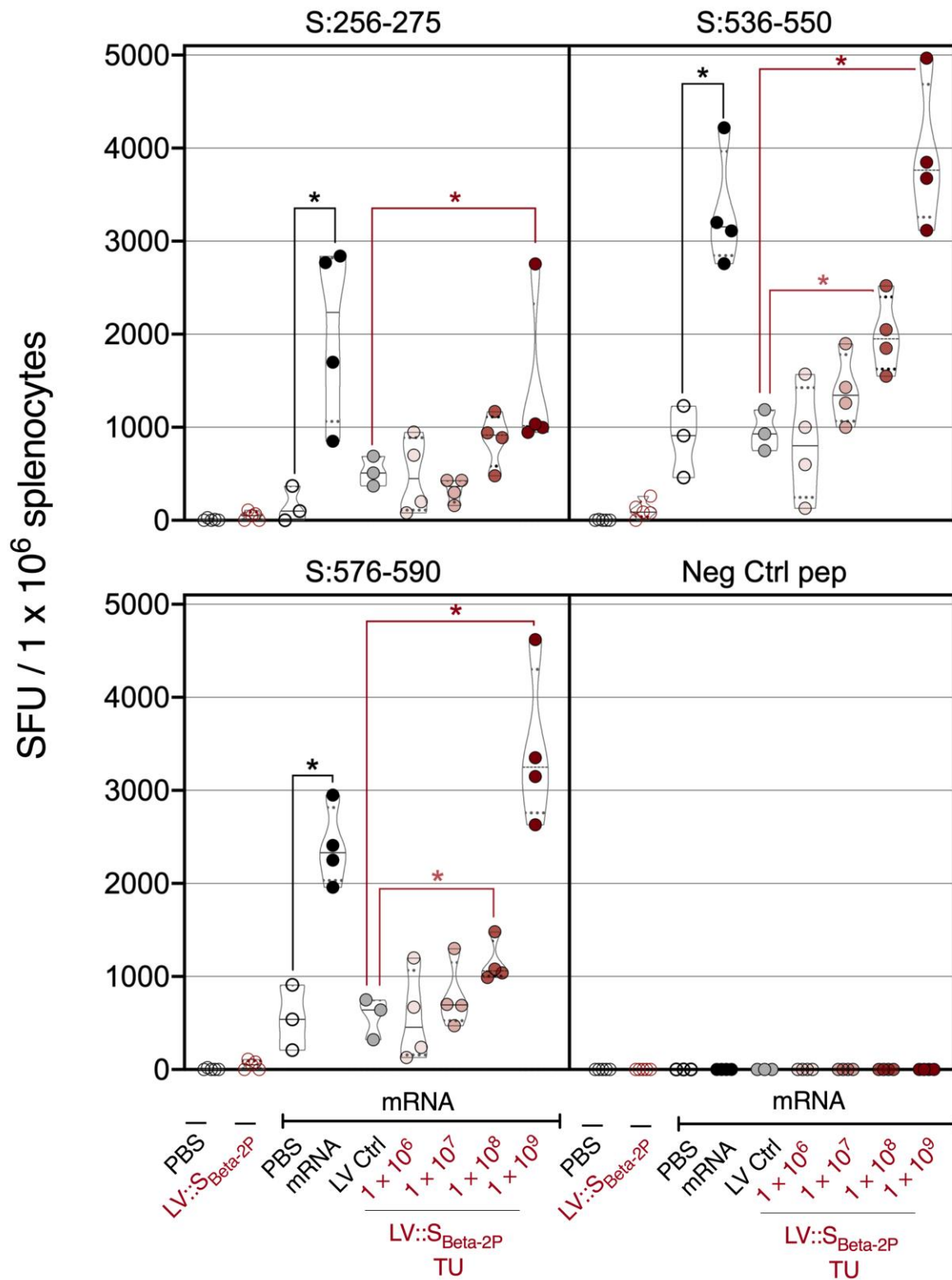
**Figure 2. Anti- $S_{CoV-2}$  humoral responses in mRNA-vaccinated mice which were further intranasally boosted with  $LV::S_{Beta-2P}$**  (A) Timeline of mRNA i.m.-i.m. prime-boost vaccination in C57BL/6 mice which were later immunized i.n. by escalating doses of  $LV::S_{Beta-2P}$  ( $n = 4-5$ /group) and the (cross) sero-neutralization follow-up. (B) Serum EC50 determined at the indicated time points against pseudo-viruses carrying  $S_{CoV-2}$  from D614G, Alpha, Beta, Gamma, Delta or Delta+ variants. (C) Anti- $S_{CoV-2}$  IgG (upper panel) or IgA (lower panel) titers in the sera two weeks after i.n.  $LV::S_{Beta-2P}$  boost. Statistical significance was determined by Mann-Whitney test (\*=  $p < 0.05$ , \*\*=  $p < 0.01$ , \*\*\*=  $p < 0.001$ ). (D) Sera EC50, after the late boost given at wk 15, and as determined at wk 17. £ = not determined.

Figure 3



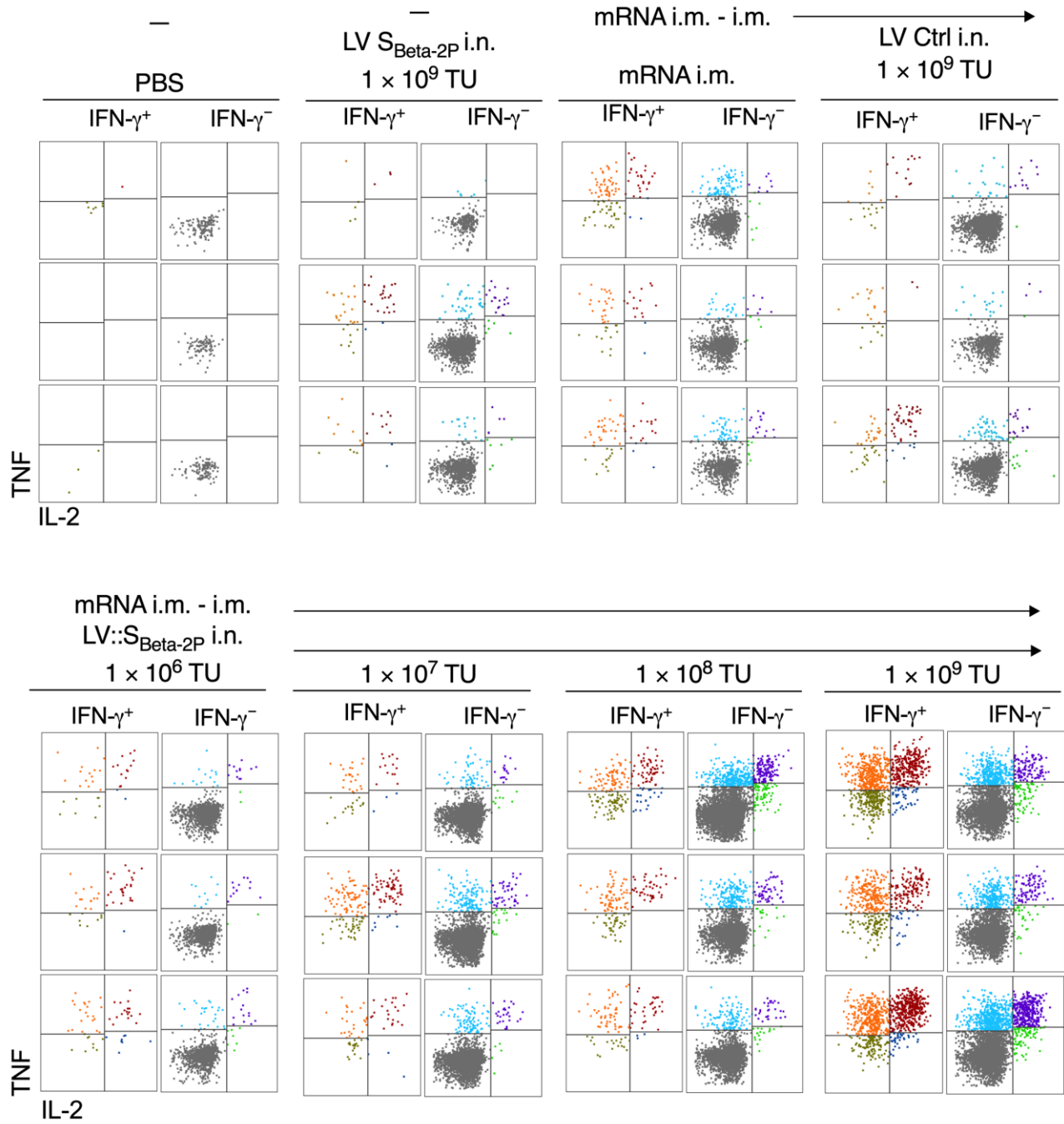
**Figure 3. Lung B-cell resident memory subset in mRNA-vaccinated mice which were further intranasally boosted with LV::S<sub>Beta-2P</sub>.** The mice are those detailed in the Figure 2. Mucosal immune cells were studied two weeks after LV::S<sub>Beta-2P</sub> i.n. boost. **(A)** Cytometric gating strategy to detect lung Brm in mRNA-vaccinated mice which were further intranasally boosted with LV::S<sub>Beta-2P</sub>. **(B)** Percentages of these cells among lung CD19<sup>+</sup> surface IgM<sup>-</sup>/IgD<sup>-</sup> B cells in mRNA-vaccinated mice which were further intranasally boosted with LV::S<sub>Beta-2P</sub>. Statistical significance was determined by Mann-Whitney test (\*=  $p < 0.05$ ).

Figure 4



**Figure 4. Systemic CD8<sup>+</sup> T-cell responses to SCoV-2 in mRNA-vaccinated mice which were further intranasally boosted with LV::S<sub>Beta-2P</sub>.** The mice are those detailed in the Figure 2. T-splenocyte responses were evaluated two weeks after LV::S<sub>Beta-2P</sub> i.n. boost by IFN- $\gamma$  ELISPOT after stimulation with S:256-275, S:536-550 or S:576-590 synthetic 15-mer peptides encompassing SCoV-2 MHC-I-restricted epitopes. Statistical significance was evaluated by Mann-Whitney test (\*=  $p < 0.05$ ).

**Figure 5**



**Figure 5. Mucosal CD8<sup>+</sup> T-cell responses to S<sub>CoV-2</sub> in mRNA-vaccinated mice which were further intranasally boosted with LV::S<sub>Beta-2P</sub>.** The mice are those detailed in the Figure 2. (A) Representative IFN-γ response by lung CD8<sup>+</sup> T cells detected by intracellular cytokine staining after in vitro stimulation with a pool of S:256-275, S:536-550 and S:576-590 peptides. Cells are gated on alive CD45<sup>+</sup> CD8<sup>+</sup> T cells.

**A**

CD3  
LD

CD4  
CD8

CD44  
CD8

CD103  
Trm  
CD69

**B**

% vs CD44

ns

\*

mRNA

PBS

LV::S<sub>Beta-2P</sub>

PBS

mRNA

LV Ctrl

1 + 10<sup>6</sup>

1 + 10<sup>7</sup>

1 + 10<sup>8</sup>

1 + 10<sup>9</sup>

LV::S<sub>Beta-2P</sub>  
TU

26

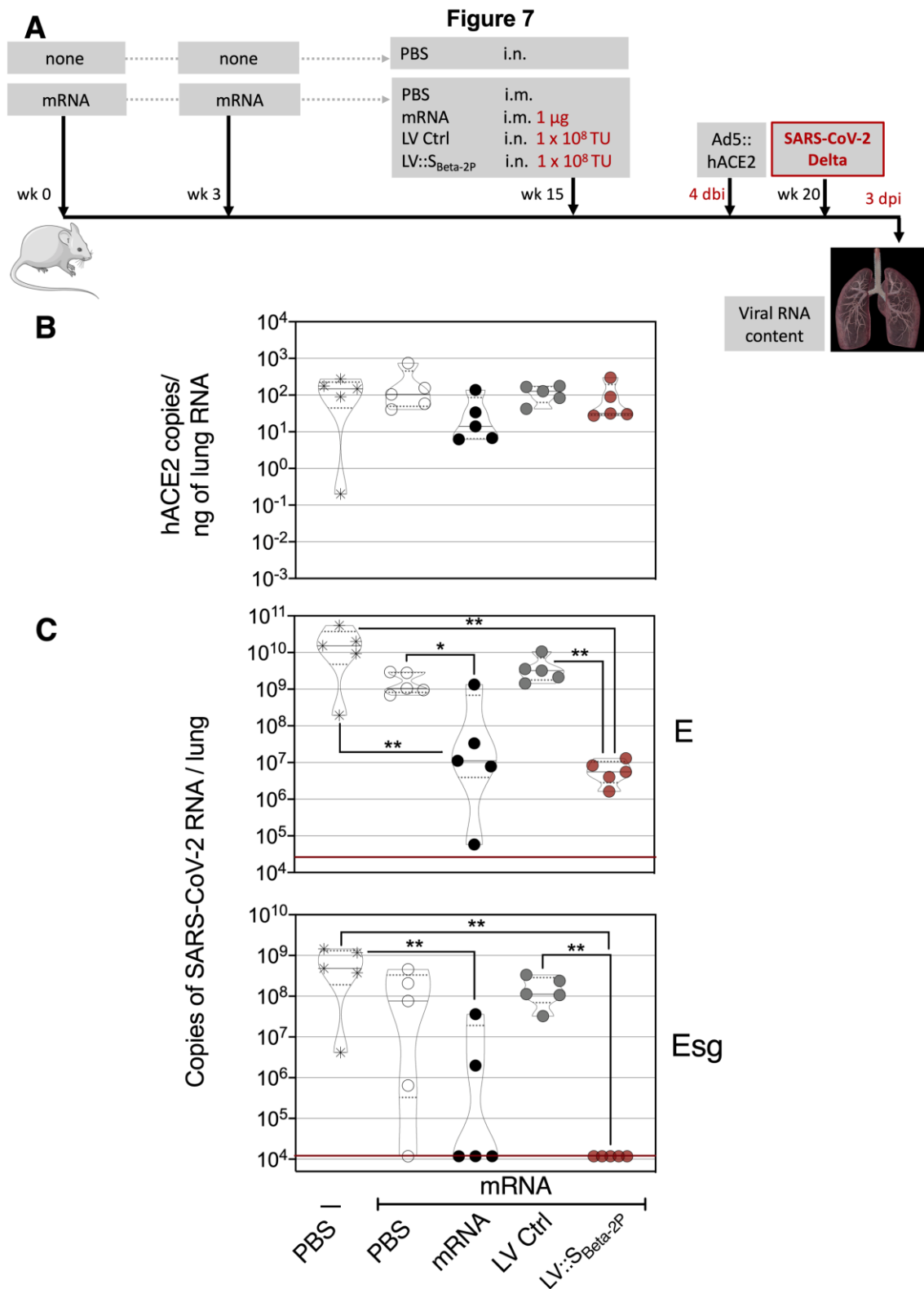


**Figure 7. Full protective capacity of LV::S<sub>Beta-2P</sub> i.n. boost against Delta variant in initially mRNA-primed and boosted mice.** (A) Timeline of mRNA i.m.-i.m. prime-boost vaccination in C57BL/6 mice which were later immunized i.n. with  $1 \times 10^8$  TU/mouse of LV::S<sub>Beta-2P</sub> ( $n = 4-5$ /group), pre-treated i.n. with Ad5::hACE-2 4 days before i.n. challenge with  $0.3 \times 10^5$  TCID<sub>50</sub> of SARS-CoV-2 Delta variant. (B) Comparative quantification of hACE-2 mRNA in the lungs of Ad5::hACE-2 pre-treated mice at 3 dpi. (C) Lung viral RNA contents, evaluated by conventional E-specific (top) or sub-genomic Esg-specific (bottom) qRT-PCR at 3 dpi. Red lines indicate the detection limits. Statistical significance was evaluated by Mann-Whitney test (\*=  $p < 0.05$ , \*\*=  $p < 0.01$ ).

Figure 8

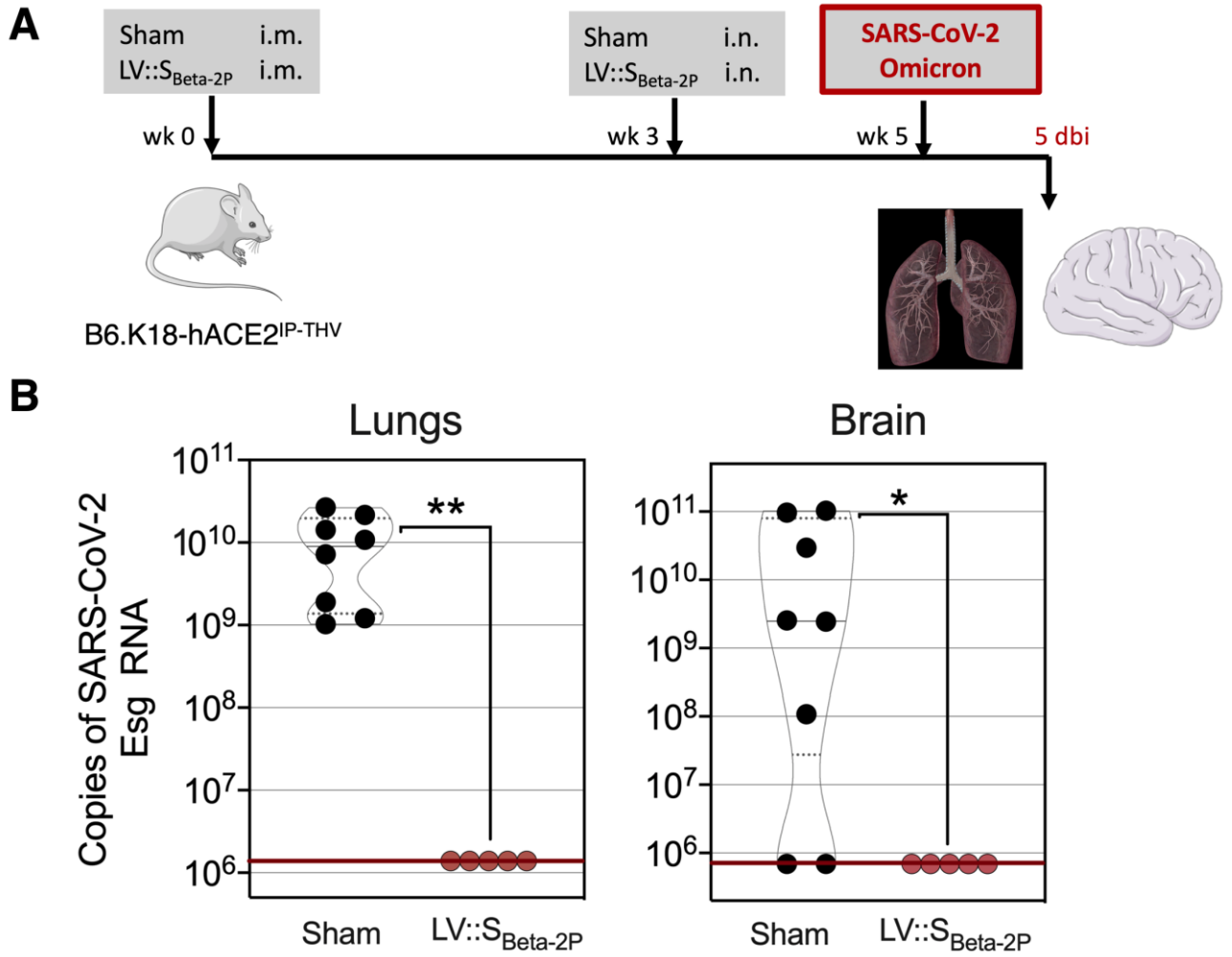


**Figure 8. Full protective capacity of LV::S<sub>Beta-2P</sub> used in a prime (i.m.) boost (i.n.) regimen against Omicron variant.** (A) Timeline of prime-boost vaccination and i.n. challenge with  $0.3 \times 10^5$  TCID<sub>50</sub> of SARS-CoV-2 Omicron variant in B6.K18-hACE2<sup>IP-THV</sup> transgenic mice ( $n = 5$ /group). (B) Lung viral RNA contents, evaluated by sub-genomic Esg-specific qRT-PCR at 5 dpi. Red lines indicate the detection limits. Statistical significance was evaluated by Mann-Whitney test (\*=  $p < 0.05$ , \*\*=  $p < 0.01$ ).